Estimating models for reference evapotranspiration with core meteorological parameters via path analysis

Ye Liu, Miao Yu, Xiaoyi Ma and Xuguang Xing

ABSTRACT

Accurate estimation and reliable universal performance of reference evapotranspiration (ET_0) obtained from a few meteorological parameters are important for the rational planning of agricultural water resources and the effective management of water in irrigated regions. Meteorological data in southern China were used to calculate ET_0 using the standard Penman–Monteith formula and determined the core decision variable (hours of sunshine, N) and the limited decision variable (relative humidity, RH) using path analysis. Estimation models using an artificial neural network and wavelet neural network were established for the Wuhan and Guangzhou meteorological stations. The statistical indices were positively correlated with the decision contribution rates to ET_0. The ET_0 values for other stations in southern China were all estimated by these models, which were trained for the Guangzhou station, and then made a total comparison with Hargreaves–Samani (HS) and Priestley–Taylor (PT) empirical ET_0 models. Error analysis indicated that the root mean square error and the mean absolute per cent error were around 0.32 mm and 5.5%, respectively, with a high coefficient of determination and Nash–Sutcliffe efficiency over 0.9, indicating that these estimating models could be applied in more regions for universal analysis with high accuracy.

Key words | decision variables, estimation accuracy, neural network, path analysis, reference evapotranspiration, universal analysis

Ye Liu
Miao Yu
Xiaoyi Ma (corresponding author)
Xuguang Xing
College of Water Resources and Architectural
    Engineering,
Northwest A&F University,
Yangling,
Shaanxi 712100,
China
E-mail: xiaoyima@vip.sina.com

INTRODUCTION

Reference evapotranspiration (ET_0) is a critical parameter for calculating evapotranspiration and estimating actual crop water requirements and is widely used for choosing an irrigation system, optimizing crop planting structure, and enriching field water balance theory. Determining the characteristics of water consumption for a crop simultaneously could provide a reliable basis for the deployment of farmland water management and the allocation of agricultural water resources (Chen 1995; Temesgen et al. 2005; Trajkovic & Kolakovic 2009b; Chang et al. 2010; Kisi et al. 2012). The estimation and prediction of ET_0 are thus very important for developing a reasonable system of field irrigation and for improving agricultural water management.

The Penman–Monteith (PM) equation is recommended by the United Nations Food and Agriculture Organization (FAO) and has been accepted universally for calculating ET_0. The FAO defines ET_0 for a hypothetical crop with an assumed height of 0.12 m, a surface resistance of 70 s m^{-1}, and an albedo of 0.23, closely resembling the reference crop canopy evapotranspiration of an extensive surface of actively growing and adequately watered green grass of uniform height (Allan et al. 1998). The PM method had higher accuracy and wider applicability than the Hargreaves–Samani and Priestley–Taylor methods, but its application was limited by the difficulty of PM calculation, the required meteorological parameters, and the incompleteness of meteorological data collected by some small weather stations (Tabari & Talaee 2011; Ngongondo et al. 2013).

New estimation models have recently been proposed with the emergence of artificial neural network (ANN)

technology (Kisi & Çimen 2009; Adeloye *et al.* 2012; Baba *et al.* 2013; Shiri *et al.* 2015a). The back propagation (BP) neural network model, currently the most mature and popular neural network, provides a powerful fault-tolerant and nonlinear approximation capability for calculation, simulation and estimation. This model has been widely used for calculating and estimating ET_0 (Kumar *et al.* 2002; Cui *et al.* 2005; Khoob 2008). The meteorological parameters that are most influential during the establishment of a network model should be chosen as the inputs of the network; recent studies suggest about four parameters (Landeras *et al.* 2008; Dai *et al.* 2009; Traore *et al.* 2010; Shiri *et al.* 2011; Huo *et al.* 2012). Model concision and universal application, however, cannot be fully implemented using these many parameters, so fewer (one or two) decisive meteorological parameters should be used to estimate ET_0 for providing a reliable theoretical basis for real-time estimation and application, especially in developing countries and regions which suffer from lack of instruments and sensors (Shiri *et al.* 2014, 2015b).

Hence, the development of more efficient ET_0 estimating models is now of great importance when only few climatic data are available (Shiri *et al.* 2013). Many mathematical methods have been used to select the determining parameters, such as regression, correlation, sensitivity and trend analyses (Beven 1979; Huo *et al.* 2004; Verstraeten *et al.* 2005; Cao *et al.* 2007; Nova *et al.* 2007; Dinpashoh *et al.* 2011; Espadafor *et al.* 2011; Zhang *et al.* 2012; Li *et al.* 2013; Talaee *et al.* 2014; Tan *et al.* 2015). Many meteorological parameters, however, are strongly correlated with ET_0 and are not completely independent of each other. Regression equations or empirical formulae with fewer variables can thus easily be ineffective when analysing data using the least squares method and so are less reliable and convincing. Path analysis can identify the direct and indirect effects from independent and dependent variables and identify the most highly interacting influences from among all parameters than can a simple correlation analysis (Tao *et al.* 2013; Sun *et al.* 2014; Ambachew *et al.* 2015; Zhang *et al.* 2016).

On the other hand, the wavelet analysis provides a useful method to decompose the observed available data, in terms of both time and frequency (Daubechies 1990). Partal (2009) utilized wavelet transform to decompose and reconstruct the climate data for ET_0 estimation. Wavelet analysis, however, focuses on determining the required components of each selected climate factor instead of choosing the core parameters from all meteorological factors, which is different from path theory. Furthermore, the established models based on wavelet analysis are difficult to popularize, largely attributed to heavy workload and difficult consistent-component decision.

In fact, many studies have analysed the selection of meteorological parameters and the estimation accuracy during the establishment of neural network models for ET_0 estimation, but most were suitable only for a limited area and were unable to obtain effective estimates when the study area expanded. The universal analysis of ET_0 estimation based on an ANN model is extremely necessary. Moreover, wavelet neural network (WNN) is a new kind of network that combines the classic ANN and the wavelet analysis, which hybridize the flexibility and learning abilities of the neural network (Zhang & Benveniste 1992; Hsieh *et al.* 2011; Ong & Zainuddin 2016; Sharma *et al.* 2016). In several recent studies, the application of the wavelet analysis coupled with neural network can improve the efficiency of the traditional ANN model (Chauhan *et al.* 2009; Falamarzi *et al.* 2014; Wang *et al.* 2015). It is valuable to establish the WNN model and compare it with the ANN model for ET_0 estimation and promotion.

When the daily meteorological data from various capital cities in southern China for 1969–2010 had been prepared as the origin data, the study first calculated the reference ET_0 values using the PM equations, applied path analysis for the ET_0 values and various meteorological parameters, analysed the strength of the interactions between the meteorological parameters, and finally selected a few core decision parameters. Meteorological stations which had the same selected parameters were merged into a group, and a base station which had the most influential corresponding decision parameters was chosen from each group. Then, the ANN and WNN models could be established by investigating the estimation accuracy and reliability with the selected meteorological parameters, the data from each base station were used to train these neural network models, and the data from the other stations were used for the estimation and universal analysis. The estimation accuracy and reliability of these models were

analysed and compared with those of some empirical equations in order to provide solid technical support for applying the model.

MATERIALS AND METHODS

Study area and data sources

China is divided into northern and southern regions by the Qinling Mountains and the Huaihe River. The southern region more urgently needs to improve land use and farming productivity due to its higher population density and smaller area of arable land. Meteorological data from various municipalities and capital cities in the south were selected for the study to raise the level of agricultural development in this region (Figure 1). Summer (June–August) meteorological data for 1969–2010 were obtained from the website of the China Meteorological Data Sharing Service System (http://cdc.nmic.cn/home.do). The data included daily hours of sunshine (N, h), average temperature (T_{mean}, °C), maximum temperature (T_{max}, °C), minimum temperature (T_{min}, °C), relative humidity (RH, %) and wind speed (U_2, m s^{-1}).

Reference evapotranspiration

The PM equations are based on the energy balance and water vapour diffusion theories and so provide a better theoretical basis and much higher accuracy than other methods for calculating ET_0 and take into account both the physiological characteristics of crops and the changes in aerodynamic parameters (Allan *et al.* 1998). The PM FAO-56 formula, recommended after years of research and improvement, is:

Penman–Monteith: ET_0

$$= \frac{0.408\Delta(R_n - G) + \gamma \dfrac{900}{T + 273} u_2(e_s - e_a)}{\Delta + \gamma(1 + 0.34u_2)} \tag{1}$$

where ET_0 is the reference evapotranspiration calculated by the PM method (mm·d^{-1}), R_n is the net radiation at the crop surface (MJ·m^{-2}·d^{-1}), G is the soil heat-flux density (MJ·m^{-2}·d^{-1}), T is the mean daily air temperature at a height of 2 m (°C), U_2 is the wind speed at 2 m (m·s^{-1}), e_s is the saturation vapour pressure (kPa), e_a is the actual vapour pressure (kPa), Δ is the slope of the vapour-pressure curve (kPa·°C^{-1}), and γ is the psychometric constant (kPa·°C^{-1}).
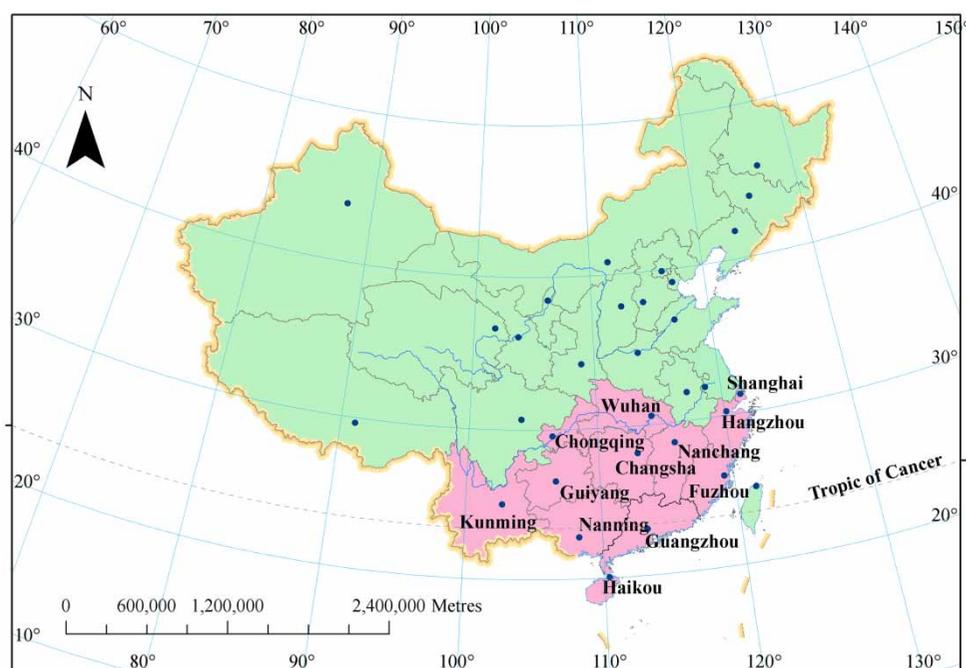

Figure 1 | Distribution of meteorological stations.

In addition, some well-known empirical models were considered to compare the performance of ET_0 calculated by the PM method. The Priestley–Taylor method (Priestley & Taylor 1972) simplified and adjusted the PM method which calculated ET_0 without RH and U_2. Moreover, the Hargreaves–Samani method (Hargreaves & Samani 1985) could compute ET_0 only by the temperature data. These two equations are listed as follows:

$$\text{Priestley–Taylor: } ET_{0PT} = \frac{1.26}{\lambda} \frac{\Delta}{\Delta + \gamma} (R_n - G) \qquad (2)$$

Hargreaves–Samani: ET_{0HS}

$$= 0.0023 \frac{R_a}{\lambda} (T_{\text{mean}} + 17.8) \sqrt{T_{\text{max}} - T_{\text{min}}} \qquad (3)$$

where ET_{0PT} is the reference evapotranspiration estimated by the Priestley–Taylor method (mm·d^{-1}), ET_{0HS} is the reference evapotranspiration estimated by the Hargreaves–Samani method (mm·d^{-1}), R_a is the daily extraterrestrial radiation (MJ·m^{-2}·d^{-1}), and λ is the latent heat of evaporation (MJ·kg^{-1}).

Path analysis theory

Path analysis was first proposed in 1921 as a mathematical and statistical method by the geneticist Sewell Wright. Nowadays, the method is broadly used in agriculture and energy demands, revealing direct or indirect relationships between some morphological characters (Mokhtassi Bidgoli *et al.* 2006; Yu *et al.* 2012; Zhang *et al.* 2016). However, little information is available on the use of this technique to evaluate the affecting factors of ET_0. Given the fact that all the meteorological variables are strongly correlated and ultimately lead to multi-collinearity, traditional trend and correlation analyses cannot quantify the interactions among the meteorological factors when filtering the suitable parameters. Path analysis is a standardized partial regression statistical technique of partitioning the correlation coefficients into direct and indirect effects, thus the direct effect and contribution of each factor to ET_0 could be calculated.

In this study, only one dependent y is ET_0 and some independents x_i are the meteorological variables. Assuming

that r_i is the simple correlation coefficient of x_i and y, r_{ij} is the simple correlation coefficient between x_i and x_j, then the canonical equations of path analysis (Stafford & Seiler 1986; Sarawgi *et al.* 1997) can be proposed as follows:

$$\begin{bmatrix} 1 & r_{12} & \cdots & r_{1n} \\ r_{21} & 1 & \cdots & r_{2n} \\ \vdots & \vdots & \ddots & \vdots \\ r_{n1} & r_{n2} & \cdots & 1 \end{bmatrix} \cdot \begin{bmatrix} P_1 \\ P_2 \\ \vdots \\ P_n \end{bmatrix} = \begin{bmatrix} r_1 \\ r_2 \\ \vdots \\ r_n \end{bmatrix} \qquad (4)$$

where P_i is the direct path coefficient, and represents the direct effects between x_i and y; $r_{ij}P_j$ is the indirect path coefficient, and shows the indirect effects of x_i on y through x_j. Another important indicator is the decision contribution rate $(R_{dc}^i = r_i P_i)$, which expresses the direct contributions of x_i on y. Hence, the key decisive parameters with the largest influence on ET_0 can be accurately obtained via the above indicators P and R_{dc}.

Artificial neural network

ANN technology provides an alternative for estimating non-linear systems including ET_0, and the feed forward BP neural network is becoming the most mature and popular ANN. Many studies have proved that the one-hidden-layer ANN model can approximate any arbitrary precision continuous function, which is generally used for estimating ET_0 in practical applications (Kumar *et al.* 2002; Landeras *et al.* 2008; Dai *et al.* 2009; Trajkovic & Kolakovic 2009a; Traore *et al.* 2010; Huo *et al.* 2012). The classical architecture of ANN applied to estimate ET_0 is composed of three layers (Figure 2): the input layer where the meteorological data chosen by the above path analysis are introduced into the model; the output layer where the reference ET_0 values calculated by the PM formulae are obtained; and the hidden layer where the network is learned and processed. The mathematical explanation of this model is given by the equations below.

$$y_k = f_1 \left(\sum_{i=1}^{n} W_{ik} x_i + \theta_k \right)$$

$$= \left[1 + \exp \left(-\sum_{i=1}^{n} W_{ik} x_i - \theta_k \right) \right]^{-1} \qquad (5)$$
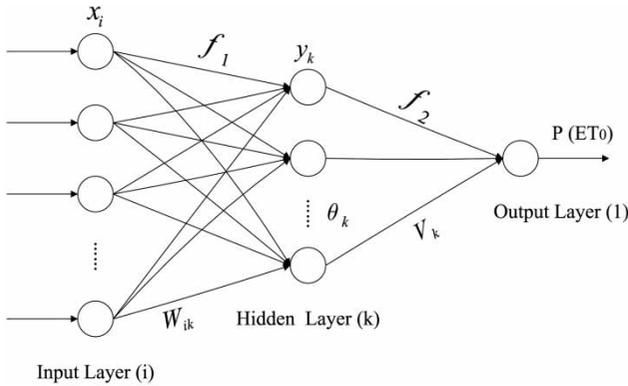
Figure 2 | Basic architecture of ANN for estimating ET_0.

$$P = f_2\left(\sum_{k=1}^{m} V_k y_k + \lambda\right) = \sum_{k=1}^{m} V_k y_k + \lambda \qquad (6)$$

where $i(1-n)$ is the ith input layer neuron and n is the number of input layer neurons; x_i is the different meteorological factors of the input layer; $k(1-m)$ is the kth hidden layer neuron and m is the number of hidden layer neurons; y_k is the input vector of the hidden layer. In addition, P is the calculation output as ET_0, and the number of output layer neurons is only 1. f is the transfer functions between the adjacent layers, including the sigmoid function $f_1(x)$ and the purelin function $f_2(x)$. The upper layer nodes and the lower layer nodes are connected by the weights W_{ik} and V_k, and the thresholds θ_k and λ.

Overall, the two steps of forward propagation of a signal and the BP of the error are executed alternately in the BP neural network model using the iterative gradient-descent technique to gradually minimize the quadratic error function defined in Equation (7). Once the target error and training parameters are established, the network model can approximate a nonlinear continuous function with any arbitrary precision by continuously correcting the network weights and thresholds.

$$E = \frac{1}{2}\sum_{n=1}^{N}(P_n - O_n)^2, \qquad (7)$$

in which P_n is the computed output by this *ANN* model, and O_n is the observed value of ET_0 calculated by the *PM* method, N is the number of training data sets.

Wavelet neural network

WNN is an ANN model constructed based on wavelet analysis. The typical architecture of WNN is shown in Figure 3. Compared with the classical ANNs, the neurons in the hidden layer are named wavelons and the activation function is a wavelet family instead of the conventional sigmoid function (Alexandridis & Zapranis 2013). A family of wavelets can be constructed from a cluster of 'mother wavelets' $\varphi(x)$, which consists of the different 'daughter wavelets' $\varphi^{a,b}(x)$ (described in Equation (8)) formed by dilation (a) and translation (b) (Chauhan *et al.* 2009). In this study, the Gaussian wavelet function defined by Equation (9) was chosen as the activation function, then the mathematical representation of the WNN model is given by Equation (10).

$$\varphi^{a,b}(x) = \frac{1}{\sqrt{a}} \cdot \varphi\left(\frac{x-b}{a}\right) \qquad (8)$$

$$\varphi(t) = -t \cdot \exp\left(-\frac{t^2}{2}\right) \qquad (9)$$

$$P = \sum_{k=1}^{m} v_k \varphi\left(\frac{\sum_{i=1}^{n} w_{ik}x_i - b_k}{a_k}\right) \qquad (10)$$

The training parameters of WNN models consist of the dilation factors a_k, the translation factors b_k, and the weight coefficients between the wavelet neurons and the input/output layer w_{ik}, v_k. These parameters were computed and adjusted during the training process, and the optimized
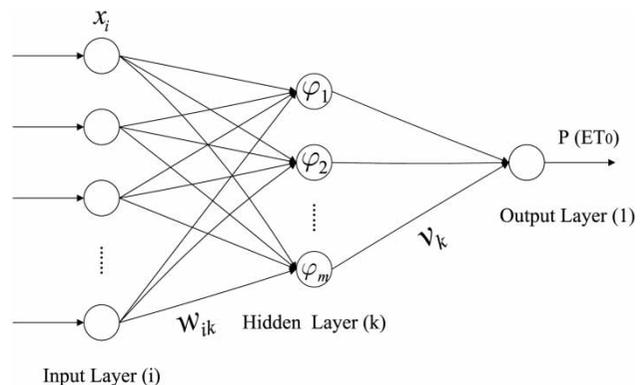

Figure 3 | Basic architecture of WNN for estimating ET_0.

values could be obtained by the same quadratic error function represented in Equation (7).

Statistical indices

Five statistical indices, root mean square error (*RMSE*), mean absolute error (*MAE*), mean absolute per cent error (*MAPE*), Nash–Sutcliffe efficiency (*NSE*) and the coefficient of determination (R^2), were selected to evaluate the efficiency of the alternative ANN models and these empirical ET_0 equations:

$$RMSE = \sqrt{\frac{1}{M}\sum_{i=1}^{M}(E_i - C_i)^2}, \tag{11}$$

$$MAE = \frac{1}{M}\sum_{i=1}^{M}|E_i - C_i|, \tag{12}$$

$$MAPE = \frac{1}{M}\sum_{i=1}^{M}\left|\frac{E_i - C_i}{C_i}\right| \times 100\%, \tag{13}$$

$$NSE = 1 - \frac{\sum_{i=1}^{M}(C_i - E_i)^2}{\sum_{i=1}^{M}(C_i - \hat{C})^2}, \tag{14}$$

and

$$R^2 = \frac{\left[\sum_{i=1}^{M}\left(C_i - \hat{C}\right)\left(E_i - \hat{E}\right)\right]^2}{\sum_{i=1}^{M}\left(C_i - \hat{C}\right)^2\sum_{i=1}^{M}\left(E_i - \hat{E}\right)^2}, \tag{15}$$

where M is the number of observed data points, E_i is ET_0 obtained by the estimated models, C_i is ET_0 calculated with the PM method, $\hat{E}$ is the average of the data arrays of E_i, and $\hat{C}$ is the average of the data arrays of C_i.

In addition, the linear regression equation $y = ax + b$ was also introduced to calibrate the performance of these estimation models. Where y is the ET_0 values calculated by the PM method, x is the ET_0 values estimated by any other empirical method or ANN model; a is the slope and b is the intercept.

RESULTS AND ANALYSES

Selection of decisive meteorological parameters

The six meteorological factors, average temperature (T_{mean}), maximum temperature (T_{max}), minimum temperature (T_{min}), relative humidity (*RH*), wind speed (U_2) and daily hours of sunshine (*N*), were strongly coupled, determining the direct influence of each parameter on ET_0 was difficult. Thus, path analysis could be implemented to detect the critical parameters. The study first calculated the correlation coefficient (*r*) between ET_0 and each meteorological parameter, then determined the direct and indirect effects of each parameter on ET_0 using the canonical equations and mathematical formulae of path analysis, and finally obtained P and R_{dc}. The analyses of the meteorological data from the Wuhan and Guangzhou stations are presented in Tables 1 and 2, respectively.

All meteorological parameters except U_2 were significantly correlated with ET_0 at the Wuhan and Guangzhou stations. The P of N was 0.7360 and 0.8216 and the R_{dc} of N was 0.7023 and 0.7985 for the Wuhan and Guangzhou stations, respectively, much higher than those for the other parameters. Thus, N was selected as the crucial decisive parameter affecting ET_0. The P and R_{dc} of RH were the highest (in absolute values) among the other five meteorological parameters, and only the P of RH was negative. Then, RH would be chosen as the second decision parameter and as the limited decisive variable. These two parameters had the most influence on ET_0, which provided a theoretical basis for the subsequent few-parameter estimation model.

Establishment of neural network models for ET_0 estimation

The meteorological parameters T_{mean}, T_{max}, T_{min}, RH, U_2 and N must all be used to calculate ET_0 by the PM equations, but N and RH were the most significant variables identified by path analysis. This study used these two decisive parameters and the calculated ET_0 values as input

Table 1 | Path analysis between meteorological parameters and ET_0 in summer at the Wuhan station

Meteorological parameter	r	Direct effect P	Indirect effect						Total	R_{dc}
			T_{mean}	T_{max}	T_{min}	RH	U_2	N		
T_{mean}	0.7585	0.1020	–	0.0220	0.0769	0.0914	0.0106	0.4556	0.6565	0.0773
T_{max}	0.8155	0.0231	0.0971	–	0.0667	0.0951	0.0106	0.5229	0.7924	0.0188
T_{min}	0.5391	0.0840	0.0934	0.0183	–	0.0657	0.0131	0.2646	0.4551	0.0453
RH	− 0.7441	− 0.1439	− 0.0648	− 0.0152	− 0.0384	–	− 0.0065	− 0.4753	− 0.6002	0.1071
U_2	0.2438	0.1282	0.0084	0.0019	0.0086	0.0073	–	0.0894	0.1156	0.0313
N	0.9542	0.7360	0.0631	0.0164	0.0302	0.0929	0.0156	–	0.2182	0.7023

Table 2 | Path analysis between meteorological parameters and ET_0 in summer at the Guangzhou station

Meteorological parameter	r	Direct effect P	Indirect effect						Total	R_{dc}
			T_{mean}	T_{max}	T_{min}	RH	U_2	N		
T_{mean}	0.7707	0.0088	–	0.0508	0.0539	0.1146	− 0.0065	0.5491	0.7618	0.0068
T_{max}	0.7899	0.0553	0.0081	–	0.0432	0.1100	− 0.0147	0.5880	0.7346	0.0437
T_{min}	0.4723	0.0660	0.0072	0.0361	–	0.0763	0.0019	0.2847	0.4062	0.0312
RH	− 0.7039	− 0.1504	− 0.0067	− 0.0404	− 0.0335	–	0.0047	− 0.4775	− 0.5535	0.1058
U_2	0.0178	0.0867	− 0.0007	− 0.0094	0.0014	− 0.0081	–	− 0.0522	− 0.0689	0.0015
N	0.9719	0.8216	0.0059	0.0396	0.0229	0.0874	− 0.0055	–	0.1502	0.7985

and output factors, respectively, using the neural network toolbox in MATLAB to establish the ANN and WNN models.

The above two estimated models with single (N) or double (N and RH) parameters were established and compared using the summer meteorological data and calculated ET_0 values for the Wuhan and Guangzhou stations for 1969–2010. The number of nodes of the corresponding hidden layer was set at three by trial-and-error to simplify and extend the utility of these models with no loss of information or data regulation. The study used the data for 1969–2003 to train the corresponding parameters and the data for 2004–2010 to validate the above models with network structures of $1 \times 3 \times 1$ and $2 \times 3 \times 1$. The total amount of water consumed during a few days in actual agricultural production, but not the daily precise consumption, was required for irrigation. The daily ET_0 was thus replaced by the 5-day average ET_0. The estimated and calculated ET_0 were then obtained. The scatterplots are shown in Figure 4,

and the statistical error indices for the estimates are listed in Table 3.

The ANN models with single (N) or double (N and RH) parameters produced reasonable and effective estimates for the Wuhan and Guangzhou stations (Figure 4 and Table 3). For the single-parameter model for the Wuhan and Guangzhou stations, the *RMSE* was 0.41 and 0.29 mm, the *MAE* was 0.32 and 0.24 mm, the *MAPE* was 6.9 and 5.4%, and the *NSE* was 0.8362 and 0.8834, respectively. The introduction of *RH* significantly reduced all error statistical indices, with *RMSE*s of 0.35 and 0.16 mm, *MAE*s of 0.24 and 0.12 mm, *MAPE*s of 5.5 and 2.9%, and *NSE*s of 0.9588 and 0.9660 for the Wuhan and Guangzhou stations, respectively. Simultaneously, the estimation situations obtained by the WNN models were very similar to the above ANN models, and the statistical indices from the WNN models were mostly superior compared with the ANN models. It could be concluded that using the Gaussian wavelet function as the activation function improved the neural
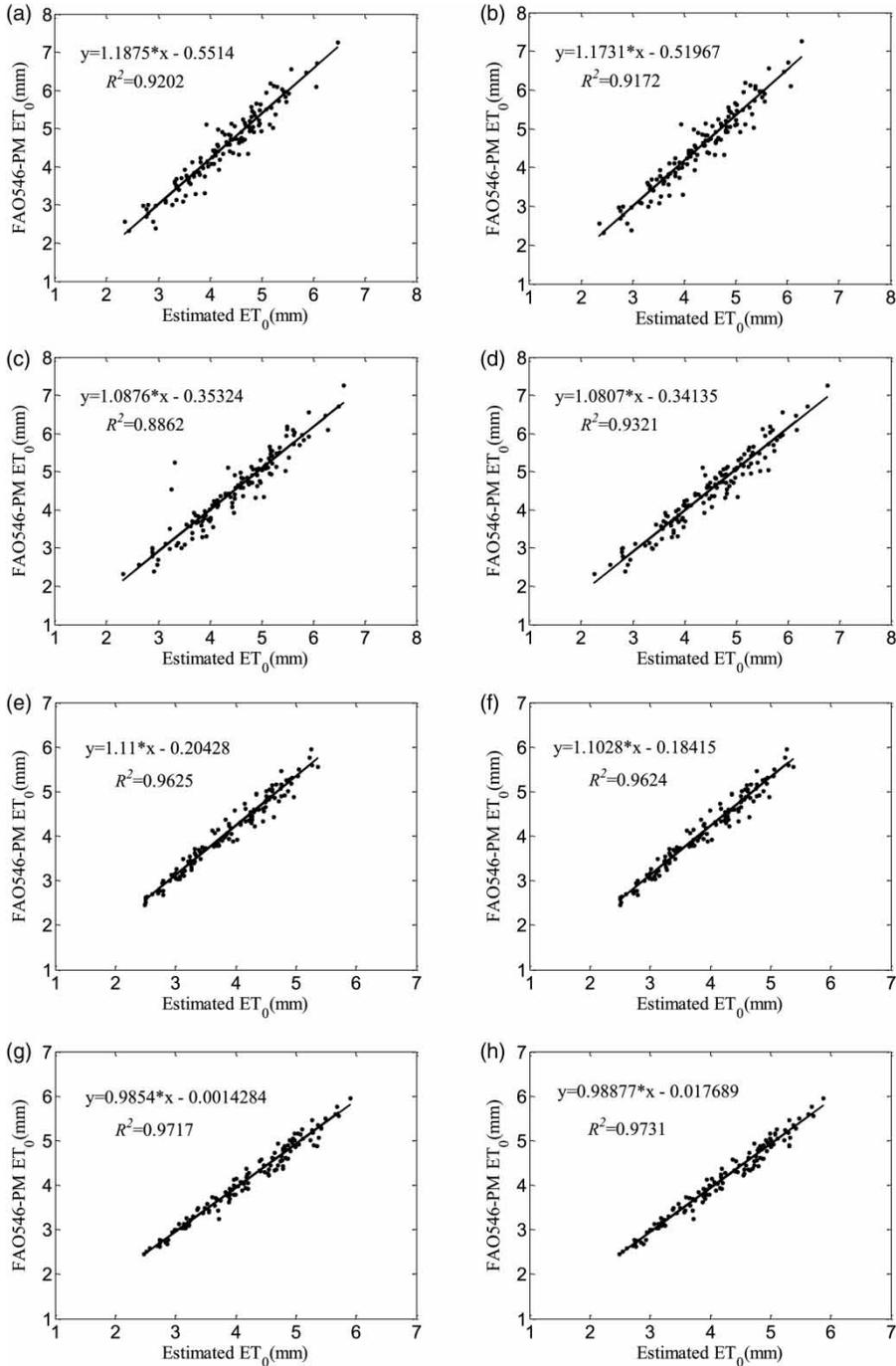
Figure 4 │ Scatter plots between calculated and estimated ET_0 using ANN and WNN models. (a) Single-factor ANN model in Wuhan. (b) Single-factor WNN model in Wuhan. (c) Double-factor ANN model in Wuhan. (d) Double-factor WNN model in Wuhan. (e) Single-factor ANN model in Guangzhou. (f) Single-factor WNN model in Guangzhou. (g) Double-factor ANN model in Guangzhou. (h) Double-factor WNN model in Guangzhou.

network model accuracy better than utilizing the basic sigmoid function, when the networks trained and validated in the same local station.

In summary, the above results indicated that all models met the requirements of good estimates and acceptable accuracy in actual application, and the double-parameter

Table 3 | Comparison of ET_0 estimated errors using the 5-day average at the Wuhan and Guangzhou stations

Station	Input parameter	Cumulative R_{dc}	RMSE (mm)	MAE (mm)	MAPE (%)	NSE
Wuhan	N	0.7023	0.4082 (0.3933)	0.3243 (0.3095)	6.9087 (6.6338)	0.8362 (0.8479)
	N, RH	0.8094	0.3510 (0.2734)	0.2412 (0.2195)	5.4931 (5.0435)	0.9588 (0.9265)
Guangzhou	N	0.7985	0.2872 (0.2804)	0.2350 (0.2292)	5.4150 (5.2944)	0.8834 (0.8889)
	N, RH	0.9043	0.1550 (0.1526)	0.1183 (0.1168)	2.8949 (2.8875)	0.9660 (0.9671)

Note: The figures outside brackets are obtained based on ANN model; the figures inside brackets are all based on WNN model.

model also greatly improved the estimation accuracy and reliability compared to the single-parameter model. The error statistics were significantly reduced and the estimates were improved with the increase of P and R_{dc}, indicating a positive correlation between them and suggesting that the meteorological parameters N and RH could be used as the inputs for these models. Both the single- and double-parameter neural network models, which produced estimation accuracies suitable for practical application, have significant potential for agricultural application, but the universal performance of these models should be studied further.

Universal analysis of the estimation models

Investigating the universality of the estimation models in multiple regions is important for improving the performance of the neural network structures and parameters. P and R_{dc} were calculated in the path analysis for all selected capital stations in the south (Tables 4 and 5, respectively). The hours of sunshine, N, which had the largest P, reaching 0.60–0.85, was selected as the core variable, and the relative humidity, RH, which was the only negative parameter and had the second largest absolute value among all parameters, was selected as the limited variable. R_{dc}, however, fluctuated between 0.53 and 0.81 when the single parameter N was selected as the input variable, so the error oscillation may be larger when applying the models on a larger scale. R_{dc} increased and maintained a range of 0.8–0.9 when RH was used as the second input variable, indicating that the double-parameter model was stable and highly credible when applied in the entire selected stations.

In summary, this study established the ANN and WNN models based on two parameters (N and RH), extracted the corresponding parameters of network structure, chose the city of Guangzhou as the benchmark station with the highest cumulative R_{dc} among all stations, and applied the data for 2004–2010 from other stations to verify and universally

Table 4 | Path coefficients between each meteorological parameter and ET_0 at the capital stations in southern China

P	T_{mean}	T_{max}	T_{min}	RH	U_2	N
Guangzhou	0.0088	0.0553	0.0660	− 0.1504	0.0867	0.8216
Nanning	0.0360	0.0686	0.0496	− 0.0929	0.0972	0.8302
Kunming	0.0387	0.0536	0.0610	− 0.1715	0.0929	0.7940
Haikou	− 0.0111	0.1400	0.0507	− 0.1435	0.0856	0.7986
Guiyang	0.0032	0.0659	0.1038	− 0.1827	0.1310	0.7423
Chongqing	0.0547	0.0043	0.0831	− 0.1620	0.1294	0.7435
Fuzhou	− 0.0376	0.1019	0.1047	− 0.2326	0.1127	0.6880
Changsha	0.0551	0.0282	0.0894	− 0.2017	0.1070	0.6825
Hangzhou	0.0355	0.0668	0.0983	− 0.2310	0.0779	0.6673
Shanghai	− 0.0969	0.1715	0.1558	− 0.2787	0.1077	0.6463
Nanchang	0.0668	0.0649	0.0707	− 0.1659	0.1060	0.6975
Wuhan	0.1020	0.0231	0.0840	− 0.1439	0.1282	0.7360

Table 5 │ Decision contribution rates (R_{dc}) between each meteorological parameter and ET_0 at the capital stations in southern China

R_{dc}	T_{mean}	T_{max}	T_{min}	RH	U_2	N	N + RH
Guangzhou	0.0068	0.0437	0.0312	0.1058	0.0015	0.7985	**0.9044**
Nanning	0.0275	0.0567	0.0154	0.0683	0.0080	0.8136	0.8820
Kunming	0.0262	0.0420	0.0082	0.1186	0.0303	0.7599	0.8785
Haikou	− 0.0082	0.1037	0.0194	0.1010	0.0044	0.7703	0.8713
Guiyang	0.0024	0.0529	0.0367	0.1456	0.0373	0.7112	0.8567
Chongqing	0.0449	0.0037	0.0486	0.1381	0.0387	0.7109	0.8490
Fuzhou	− 0.0296	0.0839	0.0587	0.1867	0.0302	0.6515	0.8382
Changsha	0.0463	0.0238	0.0596	0.1763	0.0276	0.6530	0.8293
Hangzhou	0.0273	0.0547	0.0520	0.1919	0.0193	0.6339	0.8258
Shanghai	− 0.0646	0.1232	0.0818	0.2148	0.0265	0.5978	0.8125
Nanchang	0.0543	0.0540	0.0454	0.1398	0.0201	0.6707	0.8105
Wuhan	0.0773	0.0188	0.0453	0.1071	0.0313	0.7023	0.8094

analyse the models. The universal results from the ANN and WNN models are presented in Tables 6 and 7, respectively.

The calculated statistical data estimated by ANN model in Table 6 indicated that the cumulative R_{dc} decreased smoothly from 0.90 to 0.80 at each station, RMSE climbed gradually from 0.14 to 0.31 mm, MAE grew modestly from 0.11 to 0.24 mm, MAPE increased slightly from 2.5 to 5.4%. R^2 remained within the excellent range of 0.928–0.973, NSE could be maintained at a level of above 0.80. In addition, the fitted equations and higher R^2 values for

all stations indicated high estimation accuracy and consistent universal performance. These results suggested that the ANN model established for the Guangzhou station based on two meteorological parameters (N and RH) had a strong regional universality in southern China.

Despite the fact that the WNN model has a higher performance of elasticity and plasticity, the universal estimation results listed in Table 7 are not as satisfactory as the traditional ANN model. Among all the stations, two-thirds of RMSE exceeded 0.30 mm, half of MAE and MAPE were

Table 6 │ Comparison of ET_0 estimated errors based on ANN model at the capital stations in southern China

Station	Cumulative R_{dc}	RMSE (mm)	MAE (mm)	MAPE (%)	NSE	Linear regression equation	R^2
Guangzhou	0.9044	0.1415	0.1121	2.6955	0.9660	$y = 0.9854x − 0.0014$	0.9717
Nanning	0.8820	0.1383	0.1023	2.4493	0.9657	$y = 1.0201x − 0.0976$	0.9664
Kunming	0.8785	0.1361	0.1113	3.2502	0.8182	$y = 0.8632x + 0.0783$	0.9531
Haikou	0.8713	0.1590	0.1239	2.6204	0.9399	$y = 1.0861x − 0.2938$	0.9615
Guiyang	0.8567	0.1511	0.1192	3.5607	0.8316	$y = 0.9297x − 0.0161$	0.9627
Chongqing	0.8490	0.1922	0.1423	3.7743	0.9683	$y = 1.0624x − 0.2981$	0.9734
Fuzhou	0.8382	0.2454	0.1845	3.8932	0.8801	$y = 1.1862x − 0.5786$	0.9568
Changsha	0.8293	0.2382	0.1844	3.9798	0.9329	$y = 1.1785x − 0.7627$	0.9608
Hangzhou	0.8258	0.2767	0.2076	4.7596	0.9204	$y = 1.1532x − 0.5945$	0.9433
Shanghai	0.8125	0.3131	0.2393	5.3582	0.8629	$y = 1.1932x − 0.6010$	0.9281
Nanchang	0.8105	0.2568	0.2000	4.1421	0.9264	$y = 1.1557x − 0.7046$	0.9459
Wuhan	0.8094	0.2583	0.2057	4.8053	0.9175	$y = 1.0999x − 0.5577$	0.9344

Table 7 | Comparison of ET_O estimated errors based on WNN model at the capital stations in southern China

Station	Cumulative R_{dc}	RMSE (mm)	MAE (mm)	MAPE (%)	NSE	Linear regression equation	R^2
Guangzhou	0.9044	0.1526	0.1168	2.8875	0.9671	$y = 0.9888x - 0.0177$	0.9731
Nanning	0.8820	0.1430	0.1060	2.5419	0.9641	$y = 1.0217x - 0.1087$	0.9652
Kunming	0.8785	0.3439	0.3042	8.9030	0.7007	$y = 0.8749x + 0.1606$	0.9539
Haikou	0.8713	0.1979	0.1426	2.9153	0.9404	$y = 1.0832x - 0.2850$	0.9604
Guiyang	0.8567	0.3245	0.2831	8.5391	0.8282	$y = 0.9359x - 0.0418$	0.9609
Chongqing	0.8490	0.2192	0.1629	4.4129	0.9654	$y = 1.0765x - 0.3550$	0.9720
Fuzhou	0.8382	0.4271	0.3309	6.2844	0.8691	$y = 1.2109x - 0.6815$	0.9543
Changsha	0.8293	0.3890	0.2933	5.7415	0.8954	$y = 1.2559x - 1.0575$	0.9509
Hangzhou	0.8258	0.3561	0.2692	5.7362	0.9061	$y = 1.1898x - 0.7432$	0.9380
Shanghai	0.8125	0.4500	0.3357	6.6770	0.8515	$y = 1.2088x - 0.6632$	0.9214
Nanchang	0.8105	0.3544	0.2663	5.2477	0.8971	$y = 1.2107x - 0.9211$	0.9330
Wuhan	0.8094	0.3114	0.2374	5.5929	0.9046	$y = 1.1399x - 0.7108$	0.9232

over 0.24 mm and 5.5%. Especially in Fuzhou and Shanghai stations, the *RMSE* and *MAE* peaked at around 0.45 mm and 0.34 mm. Furthermore, for the Kunming and Guiyang stations, the *MAPE* soared to 8.9% and 8.5%, the *NSE* dropped to 0.70 and 0.82. Given that the fitting equation slope *a* was less than 1 and the intercept *b* was very close to 0, it could be inferred that the WNN model overestimated the ET_O values partly attributed to the higher latitude values in these two cities. Fortunately, the fitted equations and R^2 values for all stations still performed well and other statistical indices ranged into an acceptable scope that could adapt the actual requirement in universal application.

Comparison of the estimation models with the empirical equations

All the validation data results from the selected 12 meteorological stations, which were calculated by the above neural network models, were mixed together and compared with some empirical models in order to further evaluate the generalization ability. The total performance of the ANN or WNN models and other empirical equations for the period of 2004–2010 are shown in Figure 5, and the statistical indices for the comparison are listed in Table 8.

Some famous empirical models for calculating ET_O are generally developed under specific agricultural conditions or using limited climate data, so that their calculated performance cannot be more accurate than the results obtained by the PM method. The Hargreaves–Samani model with only temperature data as inputs, presented the poorest performance with the *RMSE, MAE, MAPE, NSE* and R^2 equal to 0.7927 mm, 0.6580 mm, 17.1346%, 0.5039 and 0.6004, respectively. All these statistical indices could be noticeably improved by adding the radiation item as the next input with using the Priestley–Taylor model, but the scatter plot in Figure 5 shows that this model overestimated most of the ET_O values, thus making the calibration process vitally necessary. While the ANN model was introduced to estimate ET_O values using only two meteorological parameters (*N* and *RH*) selected by path analysis, the performances were tremendously improved by comparison of the empirical models, at the values of 0.3152 mm, 0.2367 mm, 5.5969%, 0.9215 and 0.9341 for *RMSE, MAE, MAPE, NSE* and R^2, respectively. For the WNN model, the *MAPE* and R^2 were slightly better than the ANN model but the other criteria were a little worse. Actually, when the estimated results are mixed together, no significant difference was found in these two models' accuracy as the per cent changes of those corresponding indices were less than 3.0%. Overall, the neural network estimated models with fewer inputs could exhibit much better accuracy in estimating ET_O values than the empirical equations. Two meteorological parameters, *N* and *RH*, detected by the theory of path analysis, were proved to be
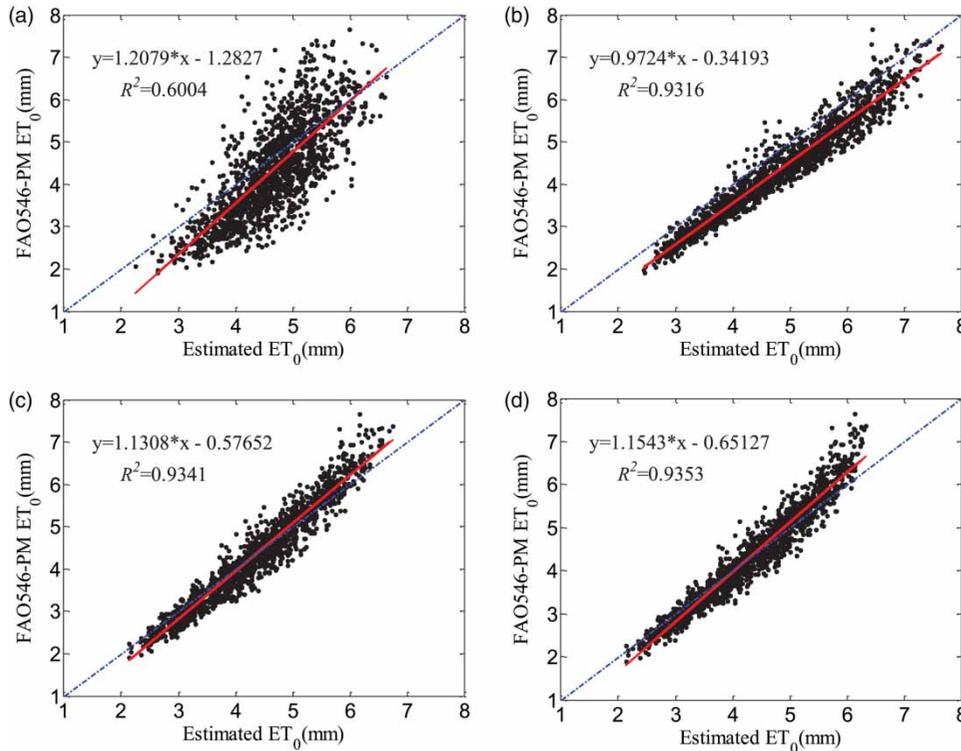
Figure 5 | Scatter plots of estimated ET_0 with different models at all the capital southern stations. (a) Hargreaves–Samani. (b) Priestley–Taylor. (c) ANN model. (d) WNN model.

Table 8 | Comparison of ET_0 estimated statistical indices using the different models at all the capital southern stations

Models	Inputs	RMSE (mm)	MAE (mm)	MAPE (%)	NSE	R^2
Hargreaves–Samani	$T_{mean}, T_{max}, T_{min}$	0.7927	0.6580	17.1346	0.5039	0.6004
Priestley–Taylor	$T_{mean}, T_{max}, T_{min}, R_s$	0.5593	0.5023	12.4166	0.7530	0.9316
ANN model	N, RH	0.3152	0.2367	5.5969	0.9215	0.9341
WNN model	N, RH	0.3215	0.2374	5.4566	0.9184	0.9353

the most crucial factors for ET_0 estimation in southern China.

DISCUSSION AND CONCLUSION

This study calculated ET_0 using the PM equations based on the summer meteorological data for 1969–2010 from 12 capital stations in southern China, determined the decisive variables N and RH using path analysis, established ANN and WNN models for estimating ET_0 to evaluate the accuracy and reliability based on actual production needs,

analysed the universal performance of the neural network models and made the comparison with some empirical equations among all stations in southern China. The following main conclusions were drawn:

1. The path analysis identified N and RH as the two core meteorological parameters with the largest influence on ET_0. N had a positive influence on ET_0 and was selected as the core decisive variable, and RH had a negative influence on ET_0 and was selected as the limited decisive variable.

2. The single-parameter (N) and the double-parameter (N and RH) neural network models based on the path theory estimated ET_0 accurately for the Wuhan and Guangzhou stations. The cumulative decision contribution rates to ET_0 were positively correlated with the error statistical indicators, demonstrating the robustness and reliability of these estimation models.

3. The double-parameter (N and RH) ANN and WNN models had the highest P and R_{dc} and the best estimation accuracy at the Guangzhou station. This local model also had higher accuracy and more consistent reliability than some empirical models when applied to other stations in southern China, confirming that this model had significant potential in agricultural applications.

In summary, the neural network estimation models with few parameters based on the principle of path analysis theory performed well, with high accuracy, consistent reliability, and robust universality. Path analysis theory thus provided a scientific basis that could feasibly be applied to choose the decisive parameters. Only two meteorological parameters (N and RH), however, could be directly applied to establish these models for estimating ET_0 for actual production, whether or not the meteorological data were fully available for some regions in southern China. Moreover, when some comparisons are made by path analysis at a large scale, it is helpful and useful to extract some stations which have the same decisive parameters into the same group in order to make further universal estimation. These concise neural network models with fewer variables have higher potential and promotional value for actual production than the empirical models, not only near the large capital cities, but also in smaller neighbouring areas.

ACKNOWLEDGEMENTS

REFERENCES

Adeloye, A. J., Rustum, R. & Kariyama, I. D. 2012 Neural computing modeling of the reference crop evapotranspiration. *Environ. Modell. Softw.* **29** (1), 61–73.

Alexandridis, A. K. & Zapranis, A. D. 2013 Wavelet neural networks: a practical guide. *Neural Networks* **42**, 1–27.

Allan, R. G., Pereira, L. S., Raes, D. & Smith, M. 1998 *Crop Evapotranspiration. Guidelines for Computing crop Water Requirements*. FAO Irrigation and Drainage Paper No. 56, FAO, Rome, Italy.

Ambachew, D., Mekbib, F., Asfaw, A., Beebe, S. E. & Blair, M. W. 2015 Trait associations in common bean genotypes grown under drought stress and field infestation by BSM bean fly. *Crop J.* **3** (4), 305–316.

Baba, A. P. A., Shiri, J., Kisi, O., Fard, A. F., Kim, S. & Amini, R. 2013 Estimating daily reference evapotranspiration using available and estimated climatic data by adaptive neuro-fuzzy inference system (ANFIS) and artificial neural network (ANN). *Hydrol. Res.* **44** (1), 131–146.

Beven, K. 1979 A sensitivity analysis of the Penman-Monteith actual evapotranspiration estimates. *J. Hydrol.* **44**, 169–190.

Cao, H. X., Su, X. L., Kang, S. Z. & Sun, H. Y. 2007 Changes of reference crop evapotranspiration and causes in Guanzhong Region of Shaanxi Province. *Trans. CSAE* **23** (11), 8–16.

Chang, F. J., Chang, L. C., Kao, H. S. & Wu, G. R. 2010 Assessing the effort of meteorological variables for evaporation estimation by self-organizing map neural network. *J. Hydrol.* **384** (1–2), 118–129.

Chauhan, N., Ravi, V. & Chandra, D. K. 2009 Differential evolution trained wavelet neural networks: application to bankruptcy prediction in banks. *Expert Syst. Appl.* **36**, 7659–7665.

Chen, Y. M. 1995 *Main Crop Water Requirement and Irrigation of China*. Water Resources and Electric Power Press, Beijing, China.

Cui, Y. L., Ma, C. X., Shen, X. Z. & Ma, J. G. 2005 Predicting reference evapotranspiration based on artificial neural network with genic arithmetic. *Adv. Water Sci.* **16**, 76–81.

Dai, X. Q., Shi, H. B., Li, Y. S., Ouyang, Z. & Huo, Z. L. 2009 Artificial neural network models for estimating regional reference evapotranspiration based on climate factors. *Hydrol. Process.* **23** (3), 442–450.

Daubechies, I. 1990 The wavelet transform, time-frequency localization and signal analysis. *IEEE T Inform. Theory* **36** (5), 961–1005.

Dinpashoh, Y., Jhajharia, D., Fakheri-Fard, A., Singh, V. P. & Kahya, E. 2011 Trends in reference crop evapotranspiration over Iran. *J. Hydrol.* **399** (3–4), 422–433.

Espadafor, M., Lorite, I. J., Gavilán, P. & Berengena, J. 2011 An analysis of the tendency of reference evapotranspiration estimates and other climate variables during the last 45 years in Southern Spain. *Agric. Water Manage.* **98** (6), 1045–1061.

Falamarzi, Y., Palizdan, N., Huang, Y. F. & Lee, T. S. 2014 Estimating evapotranspiration from temperature and wind

speed data using artificial and wavelet neural networks (WNNs). *Agric. Water Manage.* **140**, 26–36.

Hargreaves, G. H. & Samani, Z. A. 1985 Reference crop evapotranspiration from temperature. *Appl. Eng. Agric.* **1**, 96–99.

Hsieh, T. J., Hsiao, H. F. & Yeh, W. C. 2011 Forecasting stock markets using wavelet transforms and recurrent neural networks: an integrated system based on artificial bee colony algorithm. *Appl. Soft. Comput.* **11** (2), 2510–2525.

Huo, Z. L., Shi, H. B., Chen, Y. X., Wei, Z. M. & Qu, Z. Y. 2004 Spatio-temporal variation and dependence analysis of ET0 in north arid and cold region. *Trans. CSAE* **20** (6), 60–63.

Huo, Z., Feng, S., Kang, S. & Dai, X. 2012 Artificial neural network models for reference evapotranspiration in an arid area of northwest China. *J. Arid Environ.* **82**, 81–90.

Khoob, A. R. 2008 Artificial neural network estimation of reference evapotranspiration from pan evaporation in a semi-arid environment. *Irrig. Sci.* **27** (1), 35–39.

Kisi, O. & Çimen, M. 2009 Evapotranspiration modelling using support vector machines. [Modélisation de l'évapotranspiration à l'aide de 'support vector machines']. *Hydrol. Sci. J.* **54** (5), 918–928.

Kisi, O., Baba, A. P. A. & Shiri, J. 2012 Generalized neuro-fuzzy models for estimating daily pan evaporation values from weather data. *ASCE J. Irrig. Drain. Eng.* **138** (4), 1–14.

Kumar, M., Raghuwanshi, N. S., Singh, R., Wallender, W. W. & Pruitt, W. O. 2002 Estimating evapotranspiration using artificial neural network. *J. Irrig. Drain. E-ASCE* **128** (4), 224–233.

Landeras, G., Ortiz-Barredo, A. & Lopez, J. J. 2008 Comparison of artificial neural network models and empirical and semi-empirical equations for daily reference evapotranspiration estimation in the Basque Country (Northern Spain). *Agric. Water Manage.* **95** (5), 553–565.

Li, Z. L., Li, Z. J., Xu, Z. X. & Zhou, X. 2013 Temporal variations of reference evapotranspiration in Heihe River basin of China. *Hydrol. Res.* **44** (5), 904–916.

Mokhtassi Bidgoli, A., Akbari, G. A., Mirhadi, M. J., Zand, E. & Soufizadeh, S. 2006 Path analysis of the relationships between seed yield and some morphological and phenological traits in safflower (*Carthamus tinctorius* L.). *Euphytica* **148** (3), 261–268.

Ngongondo, C., Xu, C., Tallaksen, L. & Alemaw, B. 2013 Evaluation of the FAO Penman–Montheith, Priestley–Taylor and Hargreaves models for estimating reference evapotranspiration in southern Malawi. *Hydrol. Res.* **44** (4), 706–722.

Nova, N. A. V., Pereira, A. B. & Shock, C. C. 2007 Estimation of reference evapotranspiration by an energy balance approach. *Biosyst. Eng.* **96** (4), 605–615.

Ong, P. & Zainuddin, Z. 2016 Calibrating wavelet neural networks by distance orientation similarity fuzzy C-means for approximation problems. *Appl. Soft. Comput.* **42**, 156–166.

Partal, T. 2009 Modelling evapotranspiration using discrete wavelet transform and neural networks. *Hydrol. Process.* **23** (25), 3545–3555.

Priestley, C. H. B. & Taylor, R. T. 1972 On the assessment of surface heat flux and evaporation using large-scale parameters. *Mon. Weather Rev.* **100**, 81–92.

Sarawgi, A. K., Rastogi, N. K. & Soni, D. K. 1997 Correlation and path analysis in rice accessions from Madhya Pradesh. *Field Crops Res.* **52**, 161–167.

Sharma, V., Yang, D. Z., Walsh, W. & Reindl, T. 2016 Short term solar irradiance forecasting using a mixed wavelet neural network. *Renew. Energ.* **90**, 481–492.

Shiri, J., Dierickx, W., Baba, A. P. A., Neamati, S. & Ghorbani, M. A. 2011 Estimating daily pan evaporation from climatic data of the state of Illinois, USA using adaptive neuro-fuzzy inference system (ANFIS) and artificial neural network (ANN). *Hydrol. Res.* **42** (6), 491–502.

Shiri, J., Nazemi, A. H., Sadraddini, A. A., Landeras, G., Kisi, O., Fard, A. F. & Marti, P. 2013 Global cross-station assessment of neuro-fuzzy models for estimating daily reference evapotranspiration. *J. Hydrol.* **480**, 46–57.

Shiri, J., Nazemi, A. H., Sadraddini, A. A., Landeras, G., Kisi, O., Fard, A. F. & Marti, P. 2014 Comparison of heuristic and empirical approaches for estimating reference evapotranspiration from limited inputs in Iran. *Comput. Electron. Agr.* **108**, 230–241.

Shiri, J., Marti, P., Nazemi, A. H., Sadraddini, A. A., Kisi, O., Landeras, G. & Fakheri Fard, A. 2015a Local vs. external training of neuro-fuzzy and neural networks models for estimating reference evapotranspiration assessed through k-fold testing. *Hydrol. Res.* **46** (1), 72.

Shiri, J., Sadraddini, A. A., Nazemi, A. H., Marti, P., Fard, A. F., Kisi, O. & Landeras, G. 2015b Independent testing for assessing the calibration of the Hargreaves-Samani equation: new heuristic alternatives for Iran. *Comput. Electron. Agr.* **117**, 70–80.

Stafford, R. E. & Seiler, G. J. 1986 Path coefficient analyses of yield components in guar. *Field Crops Res.* **14**, 171–179.

Sun, S., Meng, P., Zhang, J., Wan, X., Zheng, N. & He, C. 2014 Partitioning oak woodland evapotranspiration in the rocky mountainous area of North China was disturbed by foreign vapor, as estimated based on non-steady-state 18O isotopic composition. *Agr. Forest Meteorol.* **184**, 36–47.

Tabari, H. & Talaee, P. H. 2011 Local calibration of the Hargreaves and Priestley-Taylor equations for estimating reference evapotranspiration in arid and cold climates of Iran based on the Penman-Monteith model. *J. Hydrol. Eng.* **16** (10), 837–845.

Talaee, P. H., Tabari, H. & Abghari, H. 2014 Pan evaporation and reference evapotranspiration trend detection in western Iran with consideration of data persistence. *Hydrol. Res.* **45** (2), 213–225.

Tan, C. L., Wong, N. H., Tan, P. Y., Jusuf, S. K. & Chiam, Z. Q. 2015 Impact of plant evapotranspiration rate and shrub albedo on temperature reduction in the tropical outdoor environment. *Build. Environ.* **94**, 206–217.

Tao, Z. Q., Chen, Y. Q., Li, C., Yuan, S.-F., Shi, J. T., Gao, W. S. & Sui, P. 2013 Path analysis between yield of spring maize and meteorological factors at different sowing times in North China Low Plain. *Acta Agron. Sin.* **39** (9), 1628–1634.

Temesgen, B., Eching, S., Davidoff, B. & Frame, K. 2005 Comparison of some reference evapotranspiration equations for California. *J. Irrig. Drain. E-ASCE* **131** (1), 73–84.

Trajkovic, S. & Kolakovic, S. 2009a Estimating reference evapotranspiration using limited weather data. *J. Irrig. Drain. E-ASCE* **135** (4), 443–449.

Trajkovic, S. & Kolakovic, S. 2009b Wind-adjusted Turc equation for estimating reference evapotranspiration at humid European locations. *Hydrol. Res.* **40** (1), 45–52.

Traore, S., Wang, Y. M. & Kerh, T. 2010 Artificial neural network for modeling reference evapotranspiration complex process in Sudano-Sahelian zone. *Agric. Water Manage.* **97** (5), 707–714.

Verstraeten, W. W., Veroustraete, F. & Feyen, J. 2005 Estimating evapotranspiration of European forests from NOAA-imagery at satellite overpass time: towards an operational processing chain for integrated optical and thermal sensor data products. *Remote Sens. Environ.* **96** (2), 256–276.

Wang, Z., Lu, F., He, H. D., Lu, Q. C., Wang, D. & Peng, Z. R. 2015 Fine-scale estimation of carbon monoxide and fine particulate matter concentrations in proximity to a road intersection by using wavelet neural network with genetic algorithm. *Atmos. Environ.* **104**, 264–272.

Yu, S. W., Zhu, K. J. & Zhang, X. 2012 Energy demand projection of China using a path-coefficient analysis and PSO-GA approach. *Energ. Convers. Manage.* **53** (1), 142–153.

Zhang, Q. & Benveniste, A. 1992 Wavelet networks. *IEEE Trans. Neural Netw.* **3** (6), 889–898.

Zhang, D. R., Zhang, L. R., Guan, Y. Q., Chen, X. & Chen, X. F. 2012 Sensitivity analysis of Xinanjiang rainfall-runoff model parameters: a case study in Lianghui, Zhejiang province, China. *Hydrol. Res.* **43** (1–2), 123–134.

Zhang, B. Z., Xu, D., Liu, Y., Li, F. S., Cai, J. B. & Du, L. J. 2016 Multi-scale evapotranspiration of summer maize and the controlling meteorological factors in north China. *Agr. Forest Meteorol.* **216**, 1–12.